Available online at www.sciencedirect.com

ScienceDirect

Mendeleev Commun., 2020, **30**, 522–524

Mendeleev Communications

Heat capacity effects associated with urea and tetramethylurea hydration: insight from computer simulation

Mikhail A. Krestyaninov and Andrey V. Kustov*

G. A. Krestov Institute of Solution Chemistry, Russian Academy of Sciences, 153045 Ivanovo, Russian Federation. E-mail: kustov@isuct.ru

DOI: 10.1016/j.mencom.2020.07.040

Molecular dynamic simulation of the hydrophilic urea and hydrophobic tetramethylurea aqueous solutions using the random network model of liquid water reveals that apolar Me groups induce an increase in the population of water molecules with linear and shorter H-bonds in their first hydration shell, whereas the carbonyl oxygen atom causes an opposite effect with elevation in the population of high angle/distance water molecules pairs. This behavior of water is the major reason for opposite changes in the heat capacity of hydration for apolar and polar species.

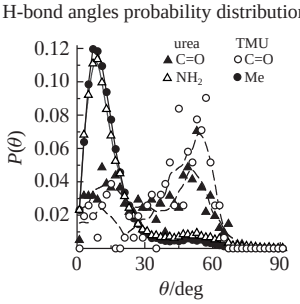

Keywords: hydrophobic and hydrophilic hydration, urea, tetramethylurea, computer simulations, angular H-bond distribution, heat capacity change.

Many of biological self-organization processes in aqueous media are known to be driven by solvent-mediated forces between hydrophobic units of associating molecules.[1–5] These so-called hydrophobic effects depend on whether the hydrophobic molecules are hydrated individually or assemble into larger structures like folded proteins, micelles or bilayer membranes.[3–6] Formation of these nano entities is determined by the size of apolar units as well as the number and distribution of polar hydrophilic moieties, which provide sufficient solubility for amphiphilic species in biological liquids. It is known that hydration of apolar solutes of a moderate molecular size is accompanied by a large positive change in heat capacity, whereas for polar groups or simple ions the change is negative.[1,5–7] These opposite signs for the heat capacities of hydration represent a hallmark of hydrophobic hydration compared with other solvation effects.[1,5] The molecular origin of hydrophobic hydration has long been a subject of interest including various models and computer simulations.[5–14] In particular, it was shown by Monte Carlo simulation[12–14] and the random network (RN) model of water[15] that apolar molecules and groups were characterized by narrower or more 'ice-like' distribution of H-bond angles as well as smaller mean length of H-bonds, which resulted in an increase in the water heat capacity in the nearest vicinity of the solute molecule. In contrast, polar groups and simple ions typically produce broader or less 'ice-like' angle distribution and larger mean length of H-bonds,[12–14] which leads to a decrease in the heat capacity of neighbour water molecules. Hydration of urea as a well-established chaotropic compound revealed the phenomenon of slight shortening and increased linearity of water–water H-bonds around amino groups compared with those for a bulk solvent.[13] This more 'ice-like' distribution of H-bond angles results in an increase in heat capacity of solvating water, which in turn leads to a positive value of heat capacity for the urea hydration process. The change in the hydration water structure previously known only for apolar solutes makes the urea behavior anomalous in this regard.

In this work, we have expanded the above approach by examination of the Extended Simple Point Charge (SPC/E) for water, two different potential functions for urea, namely the Optimized Potentials for Liquid Simulations (OPLS) and the Kirkwood–Boff Force Field (KFF) potential as well as compared the results with those for hydrophobic *N*,*N*,*N*′,*N*′-tetramethylurea (TMU) to shed light on the net effects contributing to the heat capacity of hydration for hydrophilic and hydrophobic species.[†]

After the molecular dynamic simulations had been carried out, the distances and angles were accumulated to produce their probability distribution functions, which were then used to calculate the three key parameters of the RN model of water,[15] namely the average oxygen–oxygen distance $<r>$, the root-mean-squared (RMS) deviation in the oxygen–oxygen distance $\sigma(r)$ and the RMS H-bond angle θ. These values are collected in Table 1 as averaged ones over the whole box for pure water or for the first hydration shell and a bulk solvent for urea and TMU solutions.

The heat capacity change associated with H-bond distortions induced by the solute was evaluated using a known set of equations.[12]

[†] Molecular dynamic simulations were carried out using a DL_POLY Classic package.[16] We applied the isothermal–isobaric (NPT) ensemble as well as cubic box with periodic boundary conditions containing 1000 water molecules or 999 water molecules and one solute molecule. SPC/E semirigid potential for water,[17] OPLS or KBFF potential for urea[18,19] and OPLS potential function[20] for TMU were employed. The instantaneous snapshot for each system was analyzed every 1000 steps. The solute–solvent atom–atom radial distribution functions g_r were calculated from the simulation configurations and the extent of the first hydration shell for each solute fragments was determined from the position of the first minimum of its g_r function. All the water molecules present within the solute first hydration shell were identified in each snapshot and the appropriate molecules were assigned to the hydration shell of closest solute fragment.[12,13] The lengths and angles of H-bonds were calculated for each pair of water molecules in the first hydration shell that formed the intrashell H-bonds. Two water molecules were considered as H-bonded if they were arranged within a distance of 3.3 Å[12,13] (for details, see Online Supplementary Materials).

Table 1 Averaged RN parameters for H-bonds between water molecules in pure water as well as in the first hydration shell of urea and TMU with corresponding individual contributions from the structural/energetic features of water to the heat capacities of solute hydration.[a]

System (Potential)	Atom or group	θ/deg	$<r>$/Å	$\sigma(r)$/Å	N_{HB}[b]	C_p^{bend}/ cal mol^{-1} K^{-1}	$C_p^{stretch}$/ cal mol^{-1} K^{-1}	C_p^{zpd}/ cal mol^{-1} K^{-1}	C_p^{vdW}/ cal mol^{-1} K^{-1}	C_p^{vib}/ cal mol^{-1} K^{-1}	C_p^{total}/ cal mol^{-1} K^{-1}
Water (SPC/E)	–	24.8	2.86	0.19	–	3.02	3.53	0.01	–0.89	5.96	11.63
Water (SPC/E)–urea (OPLS)	O	38.3	2.87	0.19	0.41	–0.14	–0.05	0.00	0.03	0.00	–0.16
	2 NH_2	22.9	2.85	0.19	11.66	0.47	0.41	0.05	1.05	0.00	1.98
Water (SPC/E)–urea (KBFF)	O	40.9	3.05	0.18	0.20	–0.08	–0.39	0.00	0.09	0.00	–0.38
	2 NH_2	18.5	2.81	0.17	10.96	1.21	3.48	0.05	2.08	0.00	6.82
Water (SPC/E)–TMU (OPLS)	O	44.6	3.07	0.17	0.15	–0.08	–0.32	0.00	0.08	0.00	–0.32
	4 Me	19.0	2.77	0.14	35.3	6.00	20.47	–0.15	12.7	0.00	39.03

[a] Upper indices for the heat capacity symbols indicate contributions from H-bond bending, stretching, zero-point distortion energy, van der Waals interactions and vibration as well as total heat capacity, respectively. [b] N_{HB} is the number of water–water H-bonds in the first hydration shell. The estimated uncertainty of model parameters computed from five independent simulations for water were 0.1, 0.01 and 0.002 for θ, $<r>$ and $\sigma(r)$, respectively.

As is seen from Table 1, the most portion of the effect originates from H-bond bending, stretching and van der Waals contributions, other terms being negligible.

The contribution from the solute–solvent interactions to the heat capacity change was deduced from computer simulations using appropriate potential functions for site–site interactions of various solute groups and water molecules. This value was found to approach zero for urea using both potential functions. However, the contribution is significant for TMU and reaches 27.5 cal mol^{-1} K^{-1} (for details, see Online Supplementary Materials). Figure 1 demonstrates the angle probability distribution $P(\theta)$ for H-bonds in pure water as well as in the first hydration shells of urea and TMU. For all instances the distribution is bimodal. The major first peak centered at *ca.* 8.5° originates from water molecules coordinated in a roughly tetrahedral fashion around a central molecule.[12] The smaller second peak at *ca.* 51° results from the occasional fifth water molecule that forms a part of coordination shell of the central one.[12,13] Thus, there exist two populations of hydrogen bonds between water molecules. The first one contains the species forming more linear and shorter H-bonds (see Figure 1). The second but still significant population contains molecules with longer and more bent H-bonds. Note that similar results were observed for TIP3P and TIP4P potential functions[12,13] (see Online Supplementary Materials).

As follows from Figure 1(*b*) and Table 1, amino groups of urea and methyl groups of TMU modulate relative height of the first peak in the same direction independently of the type of potential function used. Hydration of these fragments is accompanied by an increase in number of water molecules with more linear hydrogen bonds in their nearest vicinity, the effect being more pronounced for the KBFF potential. In contrast, the carbonyl oxygen atom modulates the relative height of both peaks in the opposite directions inducing an increase in the water molecules population with nonlinear H-bonds. It is seen that the key RN model parameters $<r>$ and θ decrease for apolar species compared with pure water and strongly increase for polar groups, the most sensitive value being the RMS H-bond angle θ (see Table 1).

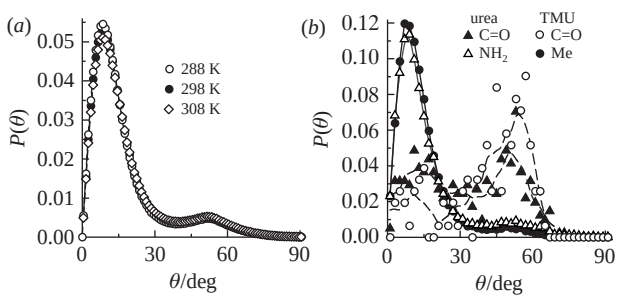

Figure 1 Probability distribution of H-bond angles: (*a*) for pure water using SPC/E potential as well as (*b*) for urea and TMU hydration shells at 298 K, both using OPLS potential. Solid lines correspond to spline functions for NH_2 and Me groups, dash lines represent smoothed data for C=O fragments.

The effect of the amino and especially methyl groups on water can be interpreted mainly in geometric terms because these moieties interact weakly with surrounding water molecules. This interplay allows the groups to retain much of their first coordination shell H-bonding geometry and displace the weakly interacting water molecules at larger $<r>$ or θ values relative to bulk solvent.[12,13] In contrast, the interplay of water molecules with the carbonyl oxygen atom is much stronger and results in radial reorientation of water dipoles and further to an increase in the population of water molecule pairs with longer and less linear H-bonds [see Figure 1(*b*)]. The calculated values of heat capacity of hydration $\Delta_{hyd}C^0$ for urea at 298 K were found to be 1.82 and 6.44 cal mol^{-1} K^{-1} for the OPLS and KBFF potentials, respectively (see Table 1). These quantities are lower than the experimental one equal to 7.4 cal mol^{-1} K^{-1}.[13] However, the agreement seems to be good taking into account the complexity of calculating the heat capacities of hydration from computer simulation data as well as our consideration of the first hydration shell only. The corresponding value for TMU is 66 cal mol^{-1} K^{-1}, which is also in good agreement with the experimental one of 77 cal mol^{-1} K^{-1}.[21,22] Analogously to other hydrophobic species such as alkanes or argon,[12–14] this value contains both contributions from the solute–solvent (27.5 cal mol^{-1} K^{-1}) and solvent–solvent (39 cal mol^{-1} K^{-1}) interactions.

Thus, relative increase in the low angle/shorter length population around apolar groups leads to an elevation of the heat capacity of water molecule pairs in their nearest vicinity, while a decrease in the population around polar groups results in an opposite effect. This change in the angular water structure has been found to involve energy fluctuations of about the right size, strongly implying that these are the causative structural effects with regard to hydration heat capacities.[14] The fluctuations are confined mainly to the first hydration shell. However, we assume that enhanced mobility of water molecules in the second hydration shell of urea[23] may originate from the structural effects observed in the first hydration shell.

In summary, our results confirm that the urea behaviour in aqueous solution is unique among polar solutes due to different mechanisms of hydration for NH_2 groups and the carbonyl oxygen atom. This behaviour seems to be independent of the potential function employed and responsible for the small though positive $\Delta_{hyd}C^0$ value for urea. Solvation of methyl groups in TMU is similar to that observed for alkanes or other hydrophobic solutes and responsible for a large heat capacity value. However, in this last case the large positive $\Delta_{hyd}C^0$ value arises not only from the solvent term, but as well originates from the pronounced temperature dependence of the TMU–water interaction energy. The behavior of water molecules nearby the C=O fragment of TMU is in turn close to that found for urea. We suppose that the

previous[12–14] and our present findings provide new insight into the molecular origin of hydrophobic effects[1–5] and shed additional light on the relationship between structural and thermodynamic properties of aqueous solutions with expected importance for protein chemistry.

This work was supported by the Russian Foundation for Basic Research (grant no. 18-03-00016a).

Online Supplementary Materials

Supplementary data associated with this article can be found in the online version at doi: 10.1016/j.mencom.2020.07.040.

References

1 K. A. Sharp, *Encyclopedia of Life Sciences*, 2001, DOI: 10.1038/npg.els.0003116.
2 L. R. Pratt, *Annu. Rev. Phys. Chem.*, 2002, **53**, 409.
3 D. Chandler, *Nature*, 2005, **437**, 640.
4 S. Rajamani, T. M. Truskett and S. Garde, *Proc. Natl. Acad. Sci. U. S. A.*, 2005, **102**, 9475.
5 A. V. Kustov, *Gidrofobnye effekty. Strukturnye, termodinamicheskie, prikladnye aspekty. Dostizheniya poslednikh let (Hydrophobic Effects. Structural, Thermodynamic, Applied Aspects. Achievements of the Last Years)*, URSS, Moscow, 2014.
6 A. V. Kustov, *Russ. J. Inorg. Chem.*, 2011, **56**, 824 (*Zh. Neorg. Khim.*, 2011, **56**, 875).
7 A. V. Kustov and N. L. Smirnova, *J. Phys. Chem. B*, 2011, **115**, 14551.
8 W. C. Swope and H. C. Andersen, *J. Phys. Chem.*, 1984, **88**, 6548.
9 S. J. Gill, S. F. Dec, G. Olofsson and I. Wadsö, *J. Phys. Chem.*, 1985, **89**, 3758.
10 Yu. M. Kessler and A. L. Zaitsev, *Solvophobic Effects*, Ellis Horwood, Chichester, 1994.
11 E. D. Kadtsyn, A. V. Anikeenko and N. N. Medvedev, *J. Mol. Liq.*, 2019, **286**, 110870.
12 B. Madan and K. Sharp, *J. Phys. Chem.*, 1996, **100**, 7713.
13 F. Vanzi, B. Madan and K. Sharp, *J. Am. Chem. Soc.*, 1998, **120**, 10748.
14 K. R. Gallagher and K. A. Sharp, *J. Am. Chem. Soc.*, 2003, **125**, 9853.
15 A. R. Henn and W. Kauzmann, *J. Phys. Chem.*, 1989, **93**, 3770.
16 W. Smith, C. W. Yong and P. M. Rodger, *Mol. Simul.*, 2002, **28**, 385.
17 H. J. C. Berendsen, J. R. Grigera and T. P. Straatsma, *J. Phys. Chem.*, 1987, **91**, 6269.
18 E. M. Duffy, D. L. Severance and W. L. Jorgensen, *Isr. J. Chem.*, 1993, **33**, 323.
19 S. Weerasinghe and P. E. Smith, *J. Phys. Chem. B*, 2003, **107**, 3891.
20 P. Belletato, L. C. G. Freitas, E. P. G. Arêas and P. S. Santos, *Phys. Chem. Chem. Phys.*, 1999, **1**, 4769.
21 A. V. Kustov and N. L Smirnova, *J. Chem. Eng. Data*, 2010, **55**, 3055.
22 A. V. Kustov, N. L. Smirnova and O. A. Antonova, *J. Chem. Thermodyn.*, 2019, **130**, 114.
23 A. Tovchigrechko, M. Rodnikova and J. Barthel, *J. Mol. Liq.*, 1999, **79**, 187.

Received: 25th February 2020; Com. 20/6140